polymers

MDPI

Article

Revealing the interface structure and bonding mechanism of coupling agent treated WPC

Jiuping Rao[a], Yonghui Zhou[a, b, 1] and Mizi Fan[a, b, 1]

[a] College of Material Engineering, Fujian Agriculture and Forestry University, Fuzhou 350002, PR China
[b] Department of Civil and Environmental Engineering, College of Engineering, Design and Physical Sciences, Brunel University London, Uxbridge, UB8 3PH, United Kingdom

Abstract: This paper presents the interfacial optimisation of wood plastic composites (WPC) based on recycled wood flour and polyethylene by employing maleated and silane coupling agents. The effect of the incorporation of the coupling agents on the variation of chemical structure of the composites were investigated by Attenuated total reflectance-Fourier Transform Infrared spectroscopy (ATR-FTIR) and Solid state ^{13}C Nuclear Magnetic Resonance spectroscopy (NMR) analyses. The results revealed the chemical reactions occurred between the coupling agents and raw materials which thus contributed to the enhancement of compatibility and interfacial adhesion between the constituents of WPC. NMR results also indicated that there existed the transformation of crystalline cellulose to an amorphous state during the coupling agent treatments, reflecting the inferior resonance of crystalline carbohydrates. Fluorescence Microscope (FM) and Scanning Electron Microscope (SEM) analyses showed the improvements of wood particle dispersion and wettability, compatibility of the constituents, and resin penetration and impregnation of the composites after the coupling agent treatments. The optimised interface of the composites was attributed to interdiffusion, electrostatic adhesion, chemical reactions and mechanical interlocking bonding mechanisms.

Keywords: wood plastic composites; interfacial optimisation; chemical reaction; adhesion; bonding mechanism.

1. Introduction

Wood plastic composites (WPC) have been considered as one of the most advanced materials, consistently growing in the last decade for uses in many industrial sectors, such as decking, automotive, siding, fencing and outdoor furniture, mainly because of the advantages that wood material possesses, namely ubiquitous availability at low cost, biorenewability and biodegradability, low density, nontoxicity, flexibility during processing, and acceptable specific strength properties [1,2]. However, inherently highly polar and hydrophilic nature of wood flour or fibre makes it incompatible with hydrophobic and non-polar matrices, especially hydrocarbon matrices (e.g. polyethylene (PE) and polypropylene (PP)) [3,4], this may cause problem in the composite processing and material performance, such as uneven distribution of the filler in the matrix and insufficient wetting of wood by the matrix, which result in weak interfacial adhesion and strength [2,5].

The interface of WPC is a heterogeneous transition zone extending from nanometers to microns with different morphological features, chemical compositions and mechanical properties [6-8]. Interfacial adhesion plays a fundamental role in the global performance of a composite. In order to formulate a reasonable WPC with optimum interface bonding, various modifications including both

[1] Corresponding authors.
Email Address: yonghui.zhou@brunel.ac.uk (Y. Zhou); fanfafu@gmail.com (M. Fan).

physical (e.g. corona, plasma, gamma radiation) and chemical approaches (e.g. alkaline, acetylation, benzoylation, peroxide, silane and maleated coupling agents treatments) have been attempted to decrease the hydrophilicity of wood flour, enhance the wettability of wood by matrix polymer, and eventually promote the interfacial adhesion of the constituents within the composite. With respect to the commercial production of WPC, incorporating coupling agents is probably the best available and feasible strategy for its interface optimisation [9].

An extensive study on the silane crosslinking of WPC and its effect on composite properties has showed that silane crosslinking can improve the adhesion between the wood filler and PE matrix by forming a set of chemical links including Si-O-C bridges, hydrogen bonds and C-C crosslinks [10-12]. As a result, the strength, toughness and creep resistance of the crosslinked composite were significantly increased. Maleated olefins, such as maleated polypropylene (MAPP) or maleated polyethylene (MAPE), had been commonly reported to enhance the compatibility and interfacial adhesion of WPC by reacting with the surface hydroxyl groups of wood through the anhydride groups of the copolymers, and at the meantime entangling with the polymer matrix through the other end of the copolymers because of their similar polarities [13-15]. The effectiveness of these coupling agent treatments were in general evaluated by the improvements in the physical and mechanical properties of the composites. Nevertheless, very few studies had paid specific attention to investigate the correlation of the chemical functionalities and reactions resulted from the coupling agent treatments with other bonding scenarios (i.e. physical and mechanical bonding), and their contribution to the bonding mechanism of the composites.

In this work, WPC materials were fabricated by the use of recycled wood flour and PE aiming at reducing the consumption of virgin raw materials and the environmental impact. The focus of this work was to optimise the interface of WPC by incorporating three different coupling agents, i.e. MAPE, bis(triethoxysilylpropyl)tetrasulfide (Si69) and vinyltrimethoxysilane (VTMS); hence to comprehensively reveal the interface structure and bonding scenarios, and unveil the chemical, physical and mechanical bonding mechanisms of the formulated WPC by carrying out a set of assessments including Attenuated total reflectance-Fourier Transform Infrared spectroscopy (ATR-FTIR) analysis, solid state ^{13}C Nuclear Magnetic Resonance spectroscopy (NMR) analysis, Scanning Electron Microscope (SEM) and Fluorescence Microscope (FM) analyses.

2. Materials and methods

2.1. Materials

Recycled wood flour used in this work was supplied by Rettenmeier Holding AG (Germany), with a bulk density of 0.285 kg/m^3, it was oven-dried at 105℃ for 24h to remove the moisture or water before use; recycled polyethylene (PE) pellet with a bulk density of 0.96 kg/m^3 and melt flow index (MFI) of 0.6g/10min at 190℃ was obtained from JFC Plastics Ltd (UK); lubricants 12-HSA (12-Hydroxyoctadecanoic acid) and Struktol TPW 709 were purchased from Safic Alcan UK Ltd (Warrington, UK); coupling agents, MAPE (500cP viscosity at 140℃, 0.5 wt% of maleic anhydride), Si69 (> 95% purity, 250℃ boiling point) and VTMS (> 98% purity, 123℃ boiling point), were purchased from Sigma-Aldrich (Dorset, UK). All the raw materials and additives were stored in a cool and dry place before uses.

2.2. Formulation of composites

The formulation of untreated and treated WPC with specific ratios was summarised in Table 1. All the composites were carefully prepared under the same processing condition as follows: the required amount of PE for each batch was first placed in a Brabender Plastograph twin-screw mixer and allowed to melt at 100 rpm and 190℃ for 2 min, and subsequently mixed with wood flour for 3 min. The lubricants and/or coupling agents were thus added into system and mixed for another 10 min. The resulted mixture was thus ground to pellets by using a Retsch cutting mill (SM 100, Germany). The ground blends were compression moulded on an electrically heated hydraulic press. Hot-press procedures involved 20 min preheating at 190℃ with no load applied followed by 10 min

compressing at the same temperature under the pressure of 9.81 MPa, and subsequently air cooling under load until the mould reached 40℃.

Table 1 Formulation of the composites.

Sample	Wood (%)	PE (%)	TPW 709 (%)	12HSA (%)	MAPE (%)	Si69 (%)	VTMS (%)
Untreated WPC	50	43	3.5	3.5	0	0	0
MAPE treated WPC	50	40	3.5	3.5	3	0	0
Si69 treated WPC	50	40	3.5	3.5	0	3	0
VTMS treated WPC	50	40	3.5	3.5	0	0	3

2.3. ATR-FTIR analysis

The FTIR spectra of the composites were recorded on a PerkinElmer Spectrum one Spectrometer equipped with diamond crystal and an incident angle of 45° was used. The atmospheric compensation function that minimises effect of atmospheric water and CO_2 on the sample spectra without the need for reference or calibration spectra. The Absolute Virtual Instrument (AVI) in PerkinElmer actively standarises instrument response to improve repeatability and protect data integrity. The instrument was operated under the following conditions: 4000 – 650 cm^{-1} wave number range, 4 cm^{-1} resolution and 16 scans. The specimen dimension was 2 mm × 2 mm × 1 mm for both untreated and coupling agent treated composites, and the average of three measurements was used.

2.4. Solid state ^{13}C NMR analysis

Solid state ^{13}C NMR analysis was conducted on a Bruker spectrometer with a Cross Polarization Magic Angle Spinning (CP-MAS) probe operating at 100 MHz. The measurements were performed at ambient probe temperature with high power decoupling. Samples were packed in zirconium oxide rotors of 7 mm diameter fitted with Kel-F caps. Spectra were acquired at the spinning rate of 6 kHz, with 4096 scans per spectrum collecting in the region between -130 ppm and 270 ppm.

2.5. SEM and FM analyses

All the composites were transversely cut by using a sliding microtome with the nominal thickness of around 25 microns for the morphological investigation of the cross sections. The SEM observation was conducted on a Leo 1430VP SEM operating at 10 kV, all the samples were conductively plated with gold by sputtering for 45 s before imaging. FM examination was conducted on a Carl Ziess Axioimager microscrope with a 100 W mercury burner, also, a green exciter-barrier filter set with 480/40 nm excitation wavelength and 510 nm emission wavelength was applied to observe the cross sections.

3. Results and discussion

3.1. Chemical structure and bonding

3.1.1. FTIR analysis

Fig.1 shows the FTIR spectra of the untreated and coupling agents treated WPC. The diagnostic feature in the spectrum of MAPE treated WPC was the occurrence of more intense bands at 1637 cm^{-1} and 1734 cm^{-1} corresponding to C=C and C=O stretching vibrations [16,17], which confirmed the introduction of C=C groups and formation of ester linkages (covalent bonding) between wood particle and maleic anhydride (MA) moiety, as the reaction shown in Fig. 2a. Carlborn et al. [18] reported that the regions of interest in the FTIR spectra of maleated polyolefins modified wood particles were the absorbance bands near 2900 cm^{-1} (CH stretching) and 1740 cm^{-1} (C=O stretching), suggesting the formation of ester linkages. A grafting index (GI) could be calculated by using the integrated areas under these peaks with the following equation:

$$GI_x = \frac{A_{x(treated)}}{A_{x(untreated)}} \quad (1)$$

Where, x represents the absorbance band at either 2900 cm^{-1} or 1740 cm^{-1}, A_x represents the integrated peak area. Accordingly, the bands of interest in the spectra of untreated and MAPE treated WPC were observed at 2915 cm^{-1} and 1734 cm^{-1}, and the calculated *GIs* were shown as follows: GI_{2915} = 1.14 and GI_{1734} = 1.09. With regards to the reported MAPE modified wood particles, the corresponding GI_{2900} and GI_{1740} at 5% MAPE were around 1.10 and 1.25, respectively [18]. The slightly higher GI_{1740} than GI_{1734} was resulted from the higher concentration of MAPE in the wood particles (5%) than that in WPC (3%). The spectral bands at 1031 cm^{-1} in both the spectra of untreated and MAPE treated WPC were assigned to C-O deformation and C-O-C stretching vibrations of the ethers [19]. The significant increase of the band intensity after the MAPE treatment should be resulted from the introduction of MA groups and the C-O-C covalent bonds formed between MA and wood particles.

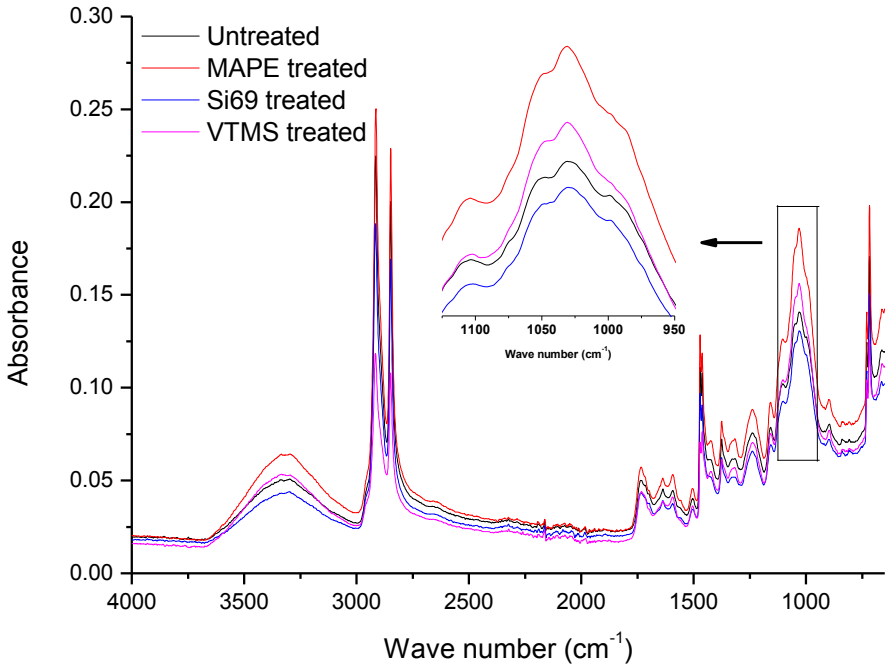

Fig. 1. FTIR spectra of untreated, MAPE, Si69 and VTMS treated WPC.

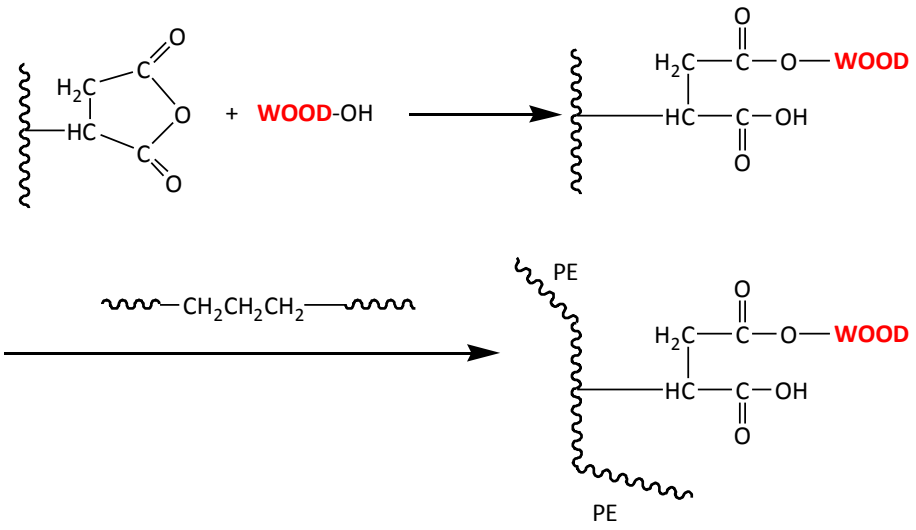

(a)

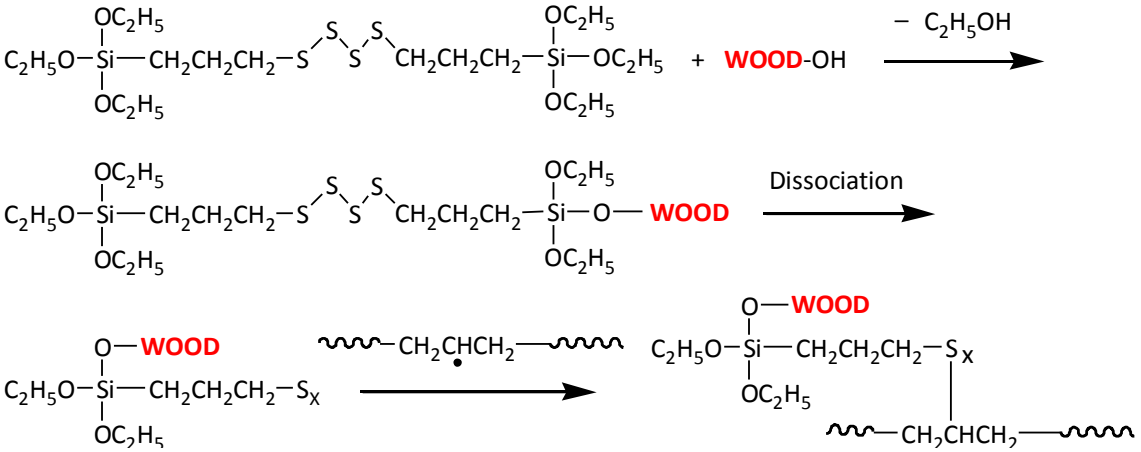

(b)

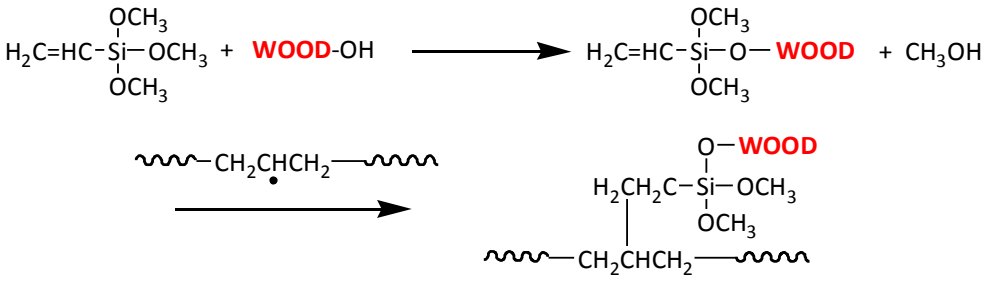

(c)

Fig. 2. Proposed chemical reactions between the coupling agents (a: MAPE; b: Si69; c: VTMS) and the raw materials of the composites.

The spectra of untreated and Si69 treated WPC did not show evident difference in terms of the band appearances and intensities, especially the bands corresponding to C-O-Si and Si-O-Si bonds (1020 cm^{-1} - 1100 cm^{-1}), which might be an indication of very limited crosslinking reaction occurred

between the coupling agent and raw materials. The disappearance of the feeble peak at 1715 cm^{-1} (C=O stretching vibration of carboxyl) and the slight shift of OH stretching vibration (shift from 3302 cm^{-1} to 3299 cm^{-1}) in the spectrum of treated WPC might be resulted from the hydrogen bonding formation between wood and hydrolysed silane (silanol). Further scrutinising of the crosslinking between Si69 and the raw materials by another analytical technique (i.e. NMR) should be of great significance for confirming the above assumptions and was carried out in the next section.

VTMS was another coupling agent applied for refining the interface of WPC. The most distinguishing characteristic presented in the spectrum of VTMS treated WPC was the strengthened intensity of the band at 1031 cm^{-1}, which was resulted from the introduced Si-O-C groups in VTMS and the Si-O-C linkages formed between wood flour and VTMS. More importantly, it might also be attributed to the formation of Si-O-Si bonds within VTMS through the hydrolysis of the methyl ether linkages and consequent condensation with adjacent silanol groups [20,21]. Compared to that of untreated WPC, the slight reduction of intensity for the band at 1101 cm^{-1} of VTMS treated WPC might be attributed to the multiple linkages of Si-O_n-Si [21]. The chemical reactions occurred between VTMS and the raw materials were proposed in Fig. 2c. VTMS was firstly reacted with hydroxyl groups in wood flour by creating covalent bonds (Wood-O-Si), the hydrophobic part of the silane on the wood surface were thus chemically bonded and/or interacted through Van der Waals force with PE molecules.

3.1.2. NMR analysis

NMR was employed to further study the effect of the incorporation of the coupling agents on the variation of chemical structure of the composites. Fig. 3 shows the comparison of the NMR spectra of untreated and treated WPC. The wood component in the composites was characterised by the spectral signals of cellulose (Fig. 4) at 105.74 ppm for C1, 89.30 ppm and 84.15 ppm for C4 of crystalline and amorphous cellulose respectively, 74.76 ppm and 72.49 ppm for C2,3,5, 65.02 ppm and 63.04 ppm for C6 of crystalline and amorphous cellulose respectively [22-27]. The diagnostic signals of hemicellulose should be at around 105 ppm (C1), 84ppm (C4), 72-75 ppm (C2,3,5), and 65 ppm (C5), which had all overlapped with the more intense signals of cellulose due to their chemical similarities [23,26]. In terms of the characteristics of lignin in wood flour, the peak observed at 172.47 ppm was assigned to carboxyl groups in lignin, peaks at 150-154 ppm and 138-132 ppm were attributed to aryl groups, and the signal at 56.3 was ascribed to methoxyl groups [22,23,26]. The resonance peaks attributed to the PE component in the composites were distinguished at the chemical shifts of 43.80 ppm and 32.51 ppm assigning to methylene groups (-CH_2-), and the comparatively subtle peaks at 26.22 ppm and 21.53 ppm were referred to methine and methyl groups respectively [27,28].

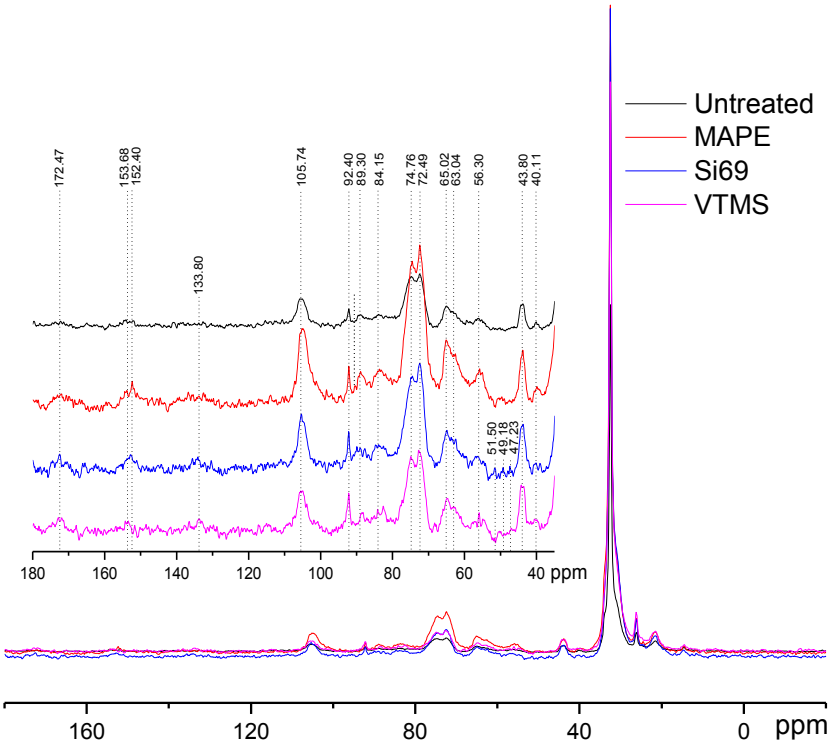

185

186 **Fig.** 3. ^{13}C NMR spectra of untreated, MAPE, Si69 and VTMS treated WPC.

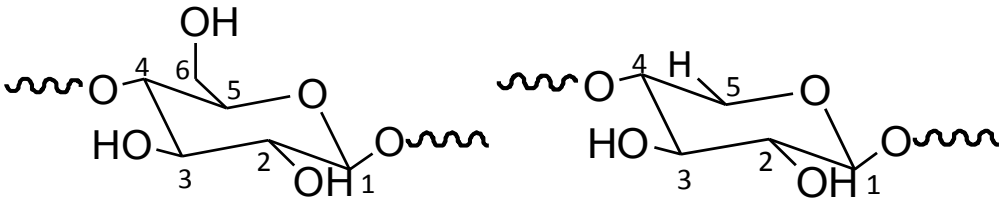

187

188

189 **Fig.** 4. Chemical structure of cellulose unit (glucose) and hemicellulose unit (xylose).

190 Regarding the resonance variations after the treatments, the first phenomenon observed was
191 that all three treated samples demonstrated broader spectra than untreated WPC, which might be
192 attributed to the less conformational exchange and rotational diffusion in the rigid phase [22]. As
193 expected, compared to the untreated counterpart, the peak intensity at 32.51 ppm in the spectrum of
194 MAPE treated sample dramatically increased, indicating that MAPE was covalently bonded to wood
195 particles. Apart from that, the more prominent signal at 172.47 ppm was not only contributed by the
196 more resolved lignin units, but should be also resulted from the introduced MA groups in MAPE and
197 ester linkages formed between the MA groups and hydroxyl groups of wood. These results were in
198 a good agreement with the above FTIR analysis of MAPE treatment. The reaction mechanism of
199 MAPE coupling agent with wood flour and PE could be explained as the activation of the copolymer
200 by heating followed by the esterification of wood particles. This treatment increases the surface
201 energy of wood flour to a level much closer to that of the matrix, and thus results in better wettability
202 and enhances interfacial adhesion between the filler and matrix [29].

203 The incorporation of Si69 into the composites were discriminated by the appearance of
204 resonance signals at 51.50 ppm, 49.18 ppm and 47.23 ppm, which were attributed to the C-Sx bonds,
205 including C-S and C-S-S existed in Si69 molecules, and the C-Sx bonds formed between the
206 dissociated coupling agent and polymer chains in the matrix (Fig. 2b) [30-32]. Compared to the spectrum
207 of the untreated sample, the new shoulder at 60.50 ppm was probably contributed by Si-O-C bonds

which existed in Si69 and covalently formed between Si69 and wood flour [33,34]. These spectral characteristics unveiled the reactions between Si69 and two constituents of the composite, which were unfortunately not discerned from FTIR analysis probably due to overlapping of diagnostic signals and insufficient concentrations of these bonds to be detected. The proposed corresponding reactions were presented in Fig. 2b. The ethoxy groups of Si69 first reacted with functional groups (mainly hydroxyl) of wood flour to form a siloxane bond, thus the sulfide group of Si69 bonded wood particle was dissociated and reacted with PE molecules to form a crosslink between wood and matrix. Si69 has a sulfidic linkage of di- to octa-sulfides and the average number of S_x- is about 3.8. Polysulfides in Si69 could be dissociated at low temperature (near room temperature) to form radicals and thus reacted with polymer molecules with storage time elapses. Therefore, the polysulfides of retained silane in the composite should be able to be dissociated and further react with both PE molecules and unreacted functional groups on wood surface [35].

In the spectrum of VTMS treated WPC, the peak at 133.80 ppm was initially assigned to lignin units in wood particles. In addition to the more resolved signal after this treatment, the strengthened intensity of this peak was also resulted from the incorporated carbons of Si-C=C and O-Si-C=C within VTMS structure [34,36]. The reaction between VTMS and wood flour (Fig. 2c) was confirmed by the occurrence of the peaks at 68 ppm and 58 ppm, since which were attributed to the carbons of Si-O-C [33,34]. The considerable enhancement of the intensity at 32.51 ppm (-CH_2-) suggested that the VTMS had successfully bonded to PE chains via its unsaturated C=C groups.

It should be pointed out that the relative resonance signals of crystalline carbohydrates (around 89 ppm and 65 ppm) to amorphous moieties (around 84 ppm and 63 ppm) decreased to some extent after the treatments, which might be an indication of the disordering of cellulose and the conversion to an amorphous state under these treatments. Transformation of crystalline cellulose to an amorphous state in hot and compressed water had been reported recently, which was determined as a consequence of synergetic effect between the thermal properties of crystalline cellulose and the unique properties of hot and compressed water [37]. It was reported that in the NMR spectra of g-methacryloxypropyl trimethoxy silane (MPS) grafted cellulose, the spectral signals of the grafted MPS and amorphous cellulose were emphasised after this silane treatment, while the crystalline cellulose form drastically decreased [38]. The possible explanation of this diminishing of relative resonance intensity of crystalline carbohydrates was that VTMS may penetrate into wood lumens and vessels, thus reacted with the functional groups of cellulose, which at the meantime underwent transformation into an amorphous form under high temperature and pressure.

3.2. Interface bonding scenarios and mechanisms

The improvement of the chemical adhesion and compatibility between the constituents of WPC resulted from the chemical bonding and reactions between the incorporated coupling agents and constituents of WPC could be anticipated to contribute to the interface refinery. The effect of the coupling agent treatment on the interface bonding scenarios of the composites was scrutinised by the use of FM and SEM (Fig. 5 and Fig. 6). It can be seen a number of clear cracks or boundaries and voids between wood particles and the matrix occurred in the untreated WPC, which indicated a poor compatibility between the untreated raw materials. It was also observed that there were agglomerated wood particles unevenly distributed in the matrix due to the readily formed hydrogen bonds within uncompatibilised wood particles [16]. In addition, although there were a few cell lumens partially filled by the polymer resin, the majorly unfilled cell lumens along with the existence of micro cracks between wood and PE denoted the improper interfacial adhesion of the untreated WPC. Comparatively, in the treated WPC (Fig. 5b-5d and Fig 6b-6d), wood flour was completely wetted by the matrix and firmly bonded to it, demonstrating superior interfacial adhesion with resin impregnation throughout the interface. More importantly, a large number of cell lumens of these samples were discerned to be partially or utterly filled by the resin, which again confirmed the enhanced interfacial adhesion and also the compatibility and wettability improvements.

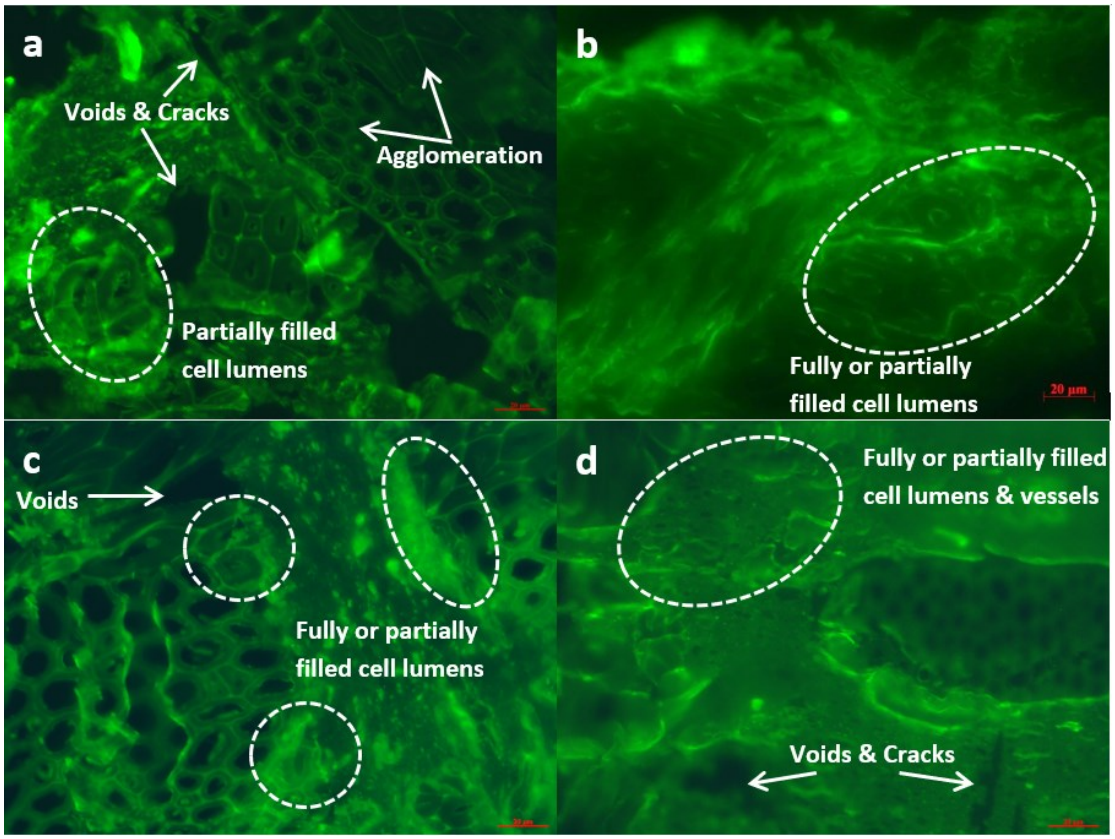

Fig. 5. FM photographs of cross section of untreated (a), MAPE treated (b), Si69 treated (c) and VTMS treated (d) composites.

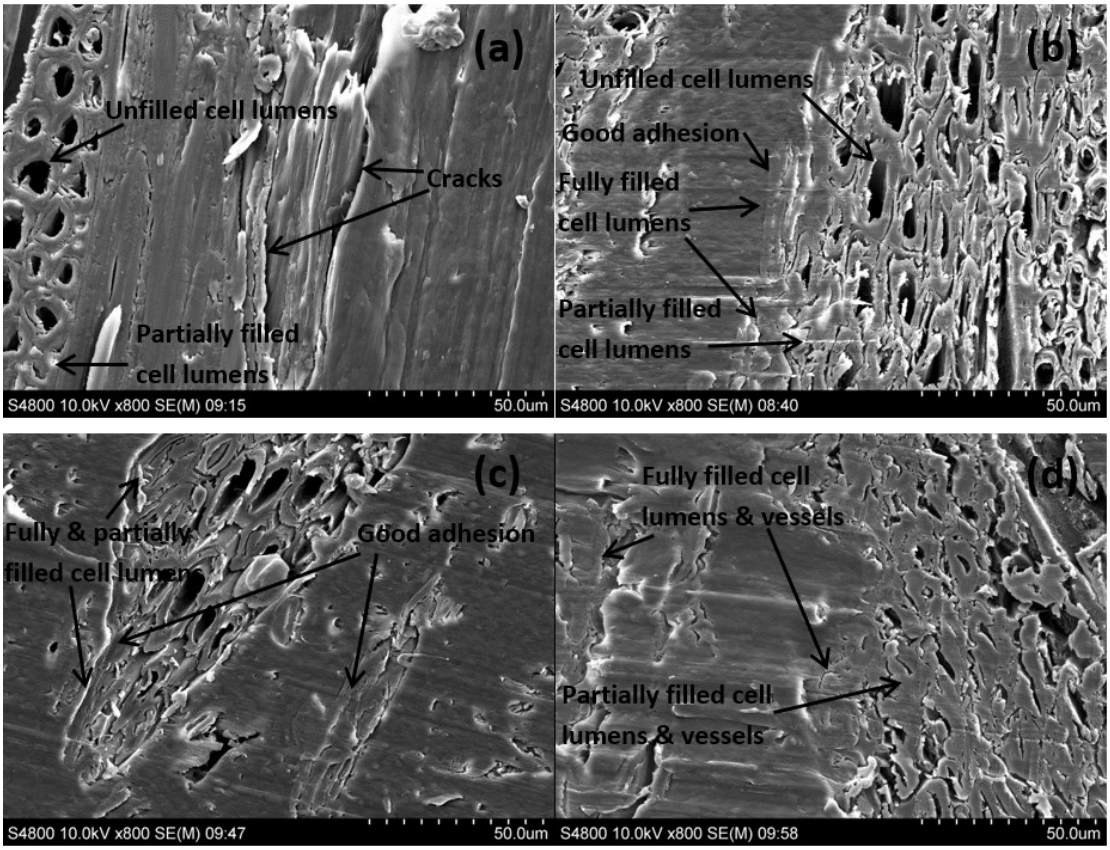

Fig. 6. SEM photographs of cross section of untreated (a), MAPE treated (b), Si69 treated (c) and VTMS treated (d) composites.

It was interesting to notice that there existed the deformed cell lumens in the treated WPC especially the VTMS treated sample (Fig. 6d), which should be resulted from the intensified pressure and compression of the interface regions during the treatments. Apart from the cell lumens, the vessels of the wood particles in VTMS treated sample were also completely or partially filled with PE resin. It was speculated that the coupling agent treatments would provide the resin with better fluidity due to the crosslinking between the hydrophobic part of coupling agent and the polymer chains of PE under high temperature and pressure, and the deformed lumens and vessels tended to facilitate the flow of resin in random directions. It has been reported that in the case of radial and tangential penetration of UF (urea-formaldehyde) adhesives into poplar wood, the resins preferably filled the wood vessels rather than the wood fibres when the wood fibres and vessels close to the bond line were deformed [39,40].

Hydrodynamic flow of molten PE resin in the composites was initiated by an external compression force through vessels, and then proceeded into the interconnected network of cell lumens and pits in interface region, with flow moving primarily in the paths of least resistance [39,40]. The flow paths in any directions were in general a combination of open cut lumens and vessels as well as of large pits.

The interface region formed between wood flour and matrix is in fact a zone of compositional, structural and property gradients, in which a set of processes occur on the atomic, microscopic and macroscopic levels. It has been recognised to play a predominant role in governing the global composite behaviour by controlling the stress transfer between wood and matrix, and is primarily dependent on the level of interfacial adhesion. The wood-matrix interfacial bonding mechanisms were assumed to include interdiffusion, electrostatic adhesion, chemical reactions and mechanical interlocking (Fig. 7), which together were responsible for the interfacial adhesion.

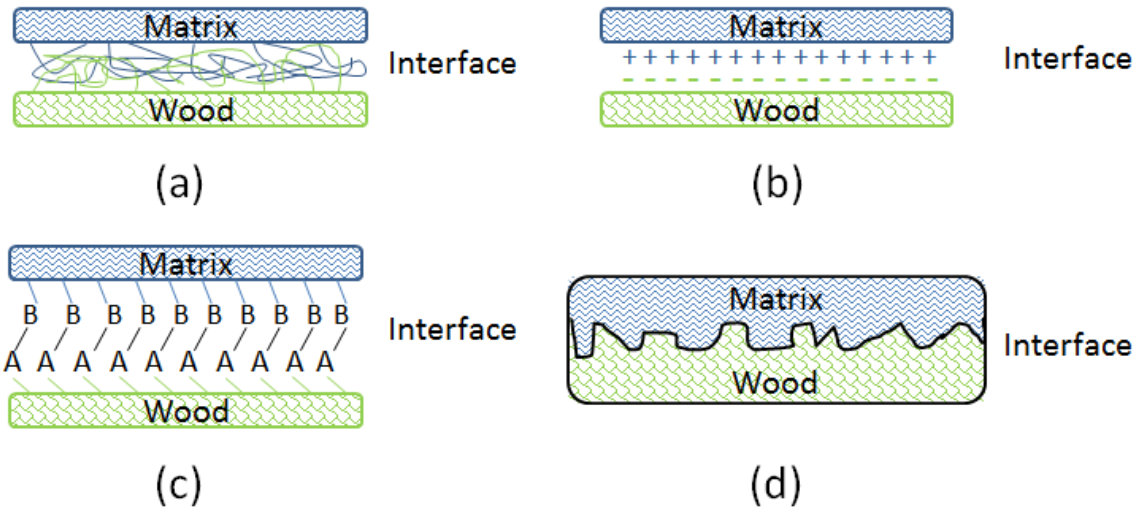

Fig. 7. Wood-matrix interfacial bonding mechanisms: (a) molecular entanglement following interdiffusion, (b) electrostatic adhesion, (c) chemical bonding and (d) mechanical interlocking.

Interdiffusion was developed on the basis of good wetting of wood particle (Fig. 6) through intimate intermolecular interactions between the molecules of wood and polymer, e.g. hydrogen and covalent bonding, electrostatic and Van der Waals forces. Electrostatic adhesion was attributed to the creation of opposite charges (anionic and cationic) on the interacting surfaces of wood and polymer matrix; thus, an interface consisting of two layers of opposite charges was formed, which accounted for the adhesion of two constituents of the composite. Chemisorption occurred when chemical bonds including atomic and ionic bonds, such as C-O-C, C-S and Si-O-C covalent bonds, were created between the substances of the composite as a result of chemical reactions. Mechanical interlocking took place through the resin penetration into the peaks, holes, valleys and crevices or other

298 irregularities of the substrate, which can be seen in the FM and SEM images (Fig. 5 and Fig. 6), then
299 anchored itself through solidification.
300 The distinguished enhancement of interfacial bonding of maleated and silane coupling agents
301 treated WPC could be explained as follows: the hydrophilic moiety in the coupling agents reacted
302 with the functional groups of wood flour to form covalent linkages, while the hydrocarbon chains
303 crosslinked with the polymer matrix to create molecular entanglements. Specifically, as thoroughly
304 discussed in the above section of chemical structure and bonding, the MA moiety in MAPE, the
305 ethoxy groups of Si69 and the methoxyl groups of VTMS reacted with the hydroxyl groups of wood
306 flour, in the meantime, the grafted PE chains in MAPE, the dissociated sulfide groups in Si69, and
307 the vinyl groups of VTMS chemically bonded and/or interacted with the PE macromolecules. Thus,
308 the extent and degree of interdiffusion between wood and PE molecules were increased due to the
309 better chemical compatibility resulted from these chemical reactions and the more flexibility of
310 interchains explored in the NMR analysis (*3.1.2*). The introduced hydrocarbon chains of coupling
311 agents also led to the decrease of hydrophilicity and the increase of surface energy of wood flour, and
312 improved the chemical affinity of the matrix, thereby resulted in enhanced wettability of the wood
313 by the resin and interfacial adhesion [29,41,42]. In addition, more contact areas between wood and matrix
314 were created for resin penetration and mechanical interlocking of the substrate (Fig. 5 and Fig. 6). The
315 more deformed cell lumens and vessels in VTMS treated sample should result in stronger mechanical
316 interlocking than MAPE and Si69 treated samples due to the increased resin penetration. In fact, an
317 increase in any bonding mechanism (i.e. interdiffusion, chemical reactions, mechanical interlocking,
318 etc.) would inevitably give rise in the enhancement of other bonding systems/mechanisms, which
319 mutually accounted for the interfacial bonding refinery.
320 The influence of the coupling agent treatments on the mechanical properties and the correlation
321 between the interface structure and performance of the composites have been comprehensively
322 studied in our previous work [43]. In short, the enhanced interfacial bonding due to the coupling agent
323 treatments resulted in improvements of bulk mechanical properties such as tensile strength, tensile
324 modulus and storage modulus, while the in situ mechanical properties of the composites were subject
325 to a number of phenomena including fibre weakening or softening impact, crystalline structure
326 transformation and cell wall deformation.

327 **4. Conclusions**

328 The interfaces of WPC were optimised by the incorporation of MAPE, Si69 and VTMS coupling
329 agents. FTIR and NMR results confirmed the chemical reactions between the coupling agents and the
330 constituents of the composites, i.e. covalent bonding with the functional groups (mainly hydroxyl
331 groups) of wood flour and crosslinking with PE molecules. The crosslinking between the coupling
332 agents and PE matrix under high temperature and pressure might give rise to better fluidity of the
333 resin and thus facilitate its hydrodynamic flow in interface region. The treated composites possessed
334 better interfacial adhesion by showing completely polymer coated wood flour, resin impregnation
335 throughout the interface, and the partially and fully resin filled cell lumens. The enhanced interface
336 of the composites after the coupling agent treatments was resulted from the combination of improved
337 interdiffusion, electrostatic adhesion, chemical reactions and mechanical interlocking.

338 **5. Acknowledgements**

339 The authors gratefully acknowledge the financial support from the European CIP-EIP-Eco-
340 innovation-2012 (Project Number: 333083).

341 **References**

342 1. Kazemi-Najafi S, Nikray SJ, Ebrahimi G. A comparison study on creep behavior of wood–plastic composite,
343 solid wood, and polypropylene. J Composite Mater 2012;46(7):801-808.

2. Xie Y, Hill CAS, Xiao Z, Militz H, Mai C. Silane coupling agents used for natural fiber/polymer composites: A review. Composites Part A 2010;41(7):806-819.

3. Bledzki AK, Gassan J, Theis S. Wood-filled thermoplastic composites. Mechanics of Composite Materials 1998;34(6):563-568.

4. Cantero G, Arbelaiz A, Llano-Ponte R, Mondragon I. Effects of fibre treatment on wettability and mechanical behaviour of flax/polypropylene composites. Composites Sci Technol 2003;63(9):1247-1254.

5. Belgacem MN, Gandini A. The surface modification of cellulose fibres for use as reinforcing elements in composite materials. Composite Interfaces 2005;12(1-2):41-75.

6. Nourbakhsh A, Ashori A. Preparation and Properties of Wood Plastic Composites Made of Recycled High-density Polyethylene. J Composite Mater 2009;43(8):877-883.

7. Lee S, Wang S, Pharr GM, Xu H. Evaluation of interphase properties in a cellulose fiber-reinforced polypropylene composite by nanoindentation and finite element analysis. Composites Part A 2007;38(6):1517-1524.

8. Lin J, Huang C, Lin Z, Lou C. Far-infrared emissive polypropylene/wood flour wood plastic composites: Manufacturing technique and property evaluations. J Composite Mater 2016;50(15):2099-2109.

9. Pickering K. *Properties and Performance of Natural-Fibre Composites*. Cambridge: Woodhead Publishing, 2008.

10. Bengtsson M, Gatenholm P, Oksman K. The effect of crosslinking on the properties of polyethylene/wood flour composites. Composites Sci Technol 2005;65(10):1468-1479.

11. Bengtsson M, Oksman K. The use of silane technology in crosslinking polyethylene/wood flour composites. Composites Part A: Applied Science and Manufacturing 2006;37(5):752-765.

12. Bengtsson M, Stark NM, Oksman K. Durability and mechanical properties of silane cross-linked wood thermoplastic composites. Composites Sci Technol 2007;67(13):2728-2738.

13. Mohanty S, Nayak SK. Interfacial, dynamic mechanical, and thermal fiber reinforced behavior of MAPE treated sisal fiber reinforced HDPE composites. J Appl Polym Sci 2006;102(4):3306-3315.

14. Mohanty S, Verma SK, Nayak SK. Dynamic mechanical and thermal properties of MAPE treated jute/HDPE composites. Composites Sci Technol 2006;66(3–4):538-547.

15. Hassaini L, Kaci M, Touati N, Pillin I, Kervoelen A, Bruzaud S. Valorization of olive husk flour as a filler for biocomposites based on poly(3-hydroxybutyrate-co-3-hydroxyvalerate): Effects of silane treatment. Polymer Testing 2017;59:430-440.

16. Osman H, Ismail H, Mustapha M. Effects of Maleic Anhydride Polypropylene on Tensile, Water Absorption, and Morphological Properties of Recycled Newspaper Filled Polypropylene/ Natural Rubber Composites. Journal of Composite Materials 2010.

17. Ihemouchen C, Djidjelli H, Boukerrou A, Fenouillot F, Barres C. Effect of compatibilizing agents on the mechanical properties of high-density polyethylene/olive husk flour composites. J Appl Polym Sci 2013;128(3):2224-2229.

18. Carlborn K, Matuana LM. Functionalization of wood particles through a reactive extrusion process. J Appl Polym Sci 2006;101(5):3131-3142.

19. Kotilainen RA, Toivanen T, Alén RJ. FTIR Monitoring of Chemical Changes in Softwood During Heating. J Wood Chem Technol 2000;20(3):307-320.

20. Ihamouchen C, Djidjelli H, Boukerrou A, Krim S, Kaci M, Martinez JJ. Effect of surface treatment on the physicomechanical and thermal properties of high-density polyethylene/olive husk flour composites. J Appl Polym Sci 2012;123(3):1310-1319.

386 21. Clemons CM, Sabo RC, Hirth KC. The effects of different silane crosslinking approaches on composites of
387 polyethylene blends and wood flour. Journal of Applied Polymer Science 2011;120(4):2292-2303.
388 22. Stael GC, D'Almeida JRM, Tavares MIB. A solid state NMR carbon-13 high resolution study of natural fiber
389 from sugar cane and their composites with EVA. Polym Test 2000;19(3):251-259.
390 23. Martins MA, Forato LA, Mattoso LHC, Colnago LA. A solid state 13C high resolution NMR study of raw and
391 chemically treated sisal fibers. Carbohydr Polym 2006;64(1):127-133.
392 24. Grünewald, T., Grigsby, W., Tondi, G., Ostrowski, S., Petutschnigg, A., Wieland,S. Chemical Characterization
393 of Wood-Leather Panels by Means of 13C NMR Spectroscopy. BioResources 2013;8(2): 2422-2452.
394 25. Renneckar SH. Modification of Wood Fiber with Thermoplastics by Reactive Steam-Explosion. PhD, Virginia
395 Polytechnic Institute and State University, 2004.
396 26. Santoni I, Callone E, Sandak A, Sandak J, Dirè S. Solid state NMR and IR characterization of wood polymer
397 structure in relation to tree provenance. Carbohydr Polym 2015;117:710-721.
398 27. Wikberg H, Liisa Maunu S. Characterisation of thermally modified hard- and softwoods by 13C CPMAS
399 NMR. Carbohydr Polym 2004;58(4):461-466.
400 28. Sombatsompop N, Sungsanit K, Thongpin C. Analysis of low-density polyethylene-g-poly(vinyl chloride)
401 copolymers formed in poly(vinyl chloride)/low-density polyethylene melt blends with gel permeation
402 chromatography and solid-state 13C-NMR. J Appl Polym Sci 2004;92(5):3167-3172.
403 29. Li X, Tabil LG, Panigrahi S. Chemical Treatments of Natural Fiber for Use in Natural Fiber-Reinforced
404 Composites: A Review. Journal of Polymers and the Environment 2007;15(1):25-33.
405 30. Zaper AM, Koenig JL. Solid-state 13C NMR studies of vulcanized elastomers, 4. Sulfur-vulcanized
406 polybutadiene. Die Makromolekulare Chemie 1988;189(6):1239-1251.
407 31. Andreis M, Liu J, Koenig JL. Solid-state carbon-13 NMR Studies of vulcanized elastomers. V. Observation of
408 new structures in sulfur-vulcanized natural rubber. Journal of Polymer Science Part B: Polymer Physics
409 1989;27(7):1389-1404.
410 32. Silverstein RM, Webster FX, Kiemle DJ, Bryce DL. Spectrometric Identification of Organic Compounds. USA:
411 Petra Recter, 2014.
412 33. Brochier Salon M, Abdelmouleh M, Boufi S, Belgacem MN, Gandini A. Silane adsorption onto cellulose fibers:
413 Hydrolysis and condensation reactions. J Colloid Interface Sci 2005;289(1):249-261.
414 34. Fyfe CA, Niu J. Direct Solid-state 13C NMR Evidence for Covalent Bond Formation between an
415 Immobilized Vinylsilane Linking Agent and Polymer Matrices Macromolecules 1995;28:3894-3897.
416 35. Choi S. Influence of storage time and temperature and silane coupling agent on bound rubber formation in
417 filled styrene–butadiene rubber compounds. Polym Test 2002;21(2):201-208.
418 36. Sitarz M, Czosnek C, Jeleń P, Odziomek M, Olejniczak Z, Kozanecki M, Janik JF. SiOC glasses produced from
419 silsesquioxanes by the aerosol-assisted vapor synthesis method. Spectrochimica Acta Part A: Molecular and
420 Biomolecular Spectroscopy 2013;112:440-445.
421 37. Deguchi S, Tsujii K, Horikoshi K. Crystalline-to-amorphous transformation of cellulose in hot and
422 compressed water and its implications for hydrothermal conversion. Green Chemistry 2008;10(2):191-196.
423 38. Salon MB, Gerbaud G, Abdelmouleh M, Bruzzese C, Boufi S, Belgacem MN. Studies of interactions between
424 silane coupling agents and cellulose fibers with liquid and solid-state NMR. Magn Reson Chem 2007;45(6):473-
425 483.

426 39. Grmusa IG, Dunky M, Miljkovic J, Momcilovic MD. Influence of the degree of condensation of urea-
427 formaldehyde adhesives on the tangential penetration into beech and fir and on the shear strength of the
428 adhesive joints. European Journal of Wood and Wood Products 2012;70(5):655-665.
429 40. Grmusa IG, Dunky M, Miljkovic J, Momcilovic MD. Influence of the viscosity of UF resins on the radial and
430 tangential penetration into poplar wood and on the shear strength of adhesive joints. Holzforschung
431 2012;66(7):849-856.
432 41. Kalaprasad G, Francis B, Thomas S, Kumar CR, Pavithran C, Groeninckx G, Thomas S. Effect of fibre length
433 and chemical modifications on the tensile properties of intimately mixed short sisal/glass hybrid fibre reinforced
434 low density polyethylene composites. Polym Int 2004;53(11):1624-1638.
435 42. Mohanty S, Nayak SK, Verma SK, Tripathy SS. Effect of MAPP as Coupling Agent on the Performance of
436 Sisal-PP Composites. J Reinf Plast Compos 2004;23(18):2047-2063.
437 43. Zhou Y, Fan M, Lin L. Investigation of bulk and in situ mechanical properties of coupling agents treated
438 wood plastic composites. Polymer Testing 2017;58:292-299.

442